Electronic Supplementary Material (ESI) for Physical Chemistry Chemical Physics.

Understanding Hydrogen Transfer Mechanism for the Biodegradation of 2,4,6-Trinitrotoluene Catalyzed by Pentaerythritol Tetranitrate Reductase: Molecular Dynamics Simulation

Supporting Information

Zhilin Yang,[†,§] ***Junxian Chen,***[‡,ǁ,§] ***Hui Huang,***[†] ***Yang Zhou,***[†,*] ***Dingguo Xu,***[‡,*] ***and Chaoyang Zhang***[†]

[†] Institute of Chemical Materials, Chinese Academy of Engineering and Physics, Mianyang 621900, P. R. China;

[‡] MOE Key Laboratory of Green Chemistry & Technology, College of Chemistry, Sichuan University, Chengdu, Sichuan 610064, P. R. China;

[ǁ] College of Chemistry and Environment Protection Engineering, SouthWest University for Nationalities, Chengdu, Sichuan, 610061, P.R. China.

*To whom Correspondence shouldbe addressed: zhouy@caep.cn (Y. Zhou) and dgxu@scu.edu.cn (D. Xu)

[§] These authors contributed equally.

Captions

Figure S1. The RESP charge distribution of $FMNH_2$ a) and TNT b) for the MD, TI, and EVB simulations.

Figure S2. a) RMSD of the backbone atoms calculated relative to the first structure in the total 40 ns MD simulation and b) The radius of gyration of all the protein atoms with the 40 ns simulation time.

Figure S3. The curves of the distance of H_{20} to different transfer sites (C_4, C_6, O_1-O_6) on TNT during the whole 20 ns MD simulations.

Figure S4. The curves of the distance of H_{21} to different transfer sites (C_4, C_6, O_1-O_6) on TNT during the whole 20 ns MD simulations.

Figure S5. The mean distance and distribution of H_{20} and H_{21} respectively to the hydrogen transfer sites (C_4, C_6, O_1, O_4, O_5) on TNT during the whole 20 ns MD simulations

Figure S6. The free energy curves of the reactions of H_{21} radical and anion transfer to O_1 atom of TNT by EVB simulations. The barrier of H_{21} radical and anion to O_1 is 27.0 kacl/mol and 28.8 kacl/mol, respectively.

Figure S7. The mean distance and standard deviation of H_{51}(Tyr351) to O_5 and O_6. The each graph shows two summits corresponding to two different mean distance in different conformations of Tyr351. The percentage of different ranges (different conformations) is also calculated.

Figure S8. The overall structure comparison between PETNR and MR, especially the residues at the active sites.

Figure S9. The comparison of the key residues (His184, Try351) between wild-type PETNR a) and His184Asn PETNR b) during the last 10 ns MD simulations.

Figure S10. H_{20} radical transfer step of TNT enzymatic reaction in the gas phase, and the intrinsic reaction coordinate (IRC) profile (B3LYP/6-31G* results) with the

indicated stationary points corresponding to the reactant (R), transition state (TS), and product (P), and the correlative activation free energy ($\Delta G^{\ddagger}$) and reaction free engergy (ΔG_R).

Table S1. Coupling parameter and weights for 7-point Gaussian integration.

Table S2. The mean distance and standard deviation of the residues polar hydrogen to oxygen of TNT in the PETNR active center.

Table S3. Non-bonded interactions energy (means and standard deviations) between residue 184 (or 351) and TNT of wild-type PETNR and His184Asn PETNR during the last 10 ns MD simulations. Elec: electrostatic energy; Vdw: van der waals energy; all the energy in kcal/mol.

Table S4. Condensed Fukui Functions of TNT. $Q_{(N)}$ is the Hirshfeld charge of TNT, $Q_{(N+1)}$ is the Hirshfeld charge of TNT combining an electron, and $Q_{(N-1)}$ is the Hirshfeld charge of TNT subtracting an electron. $f_A^0=(Q_{(N-1)}+Q_{(N+1)})/2$ corresponds to the ability of free-radical attack.

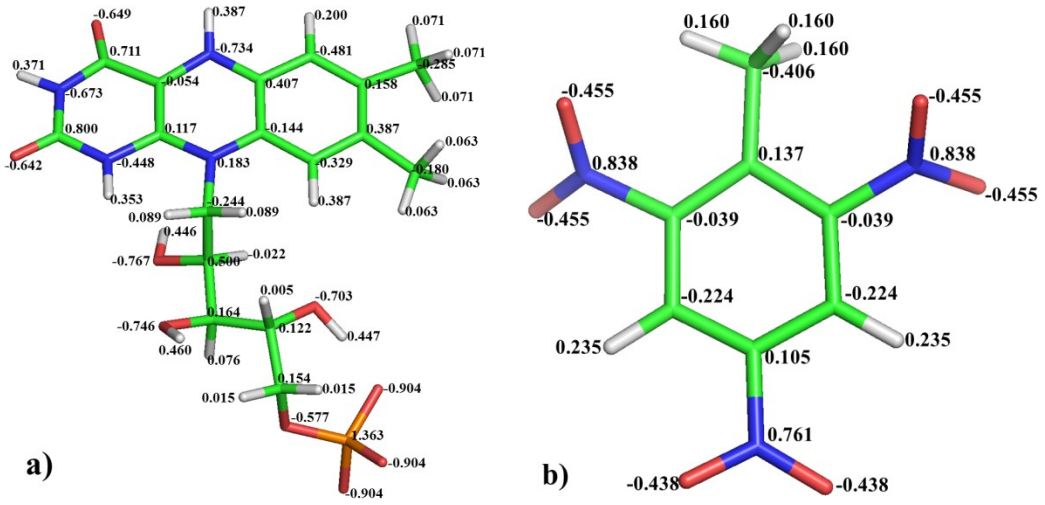

Figure S1. The RESP charge distribution of $FMNH_2$ a) and TNT b) for the MD, TI, and EVB simulations.

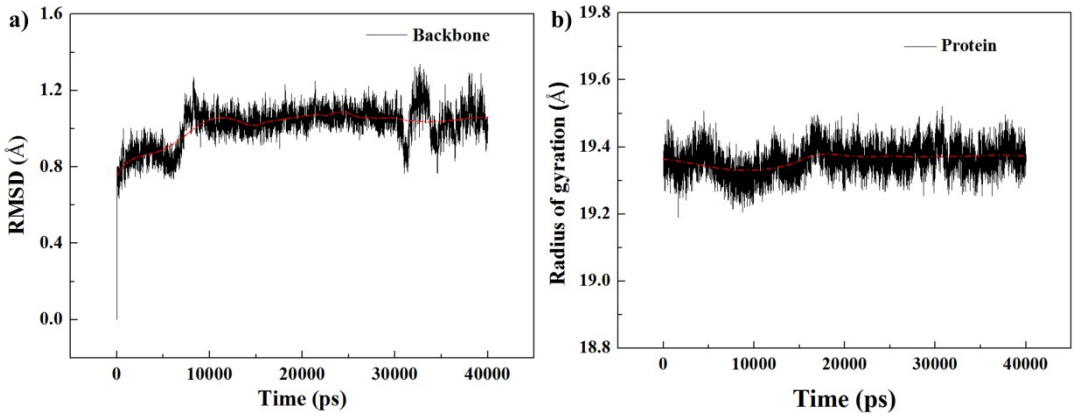

Figure S2. a) RMSD of the backbone atoms calculated relative to the first structure in the total 40 ns MD simulation and b) The radius of gyration of all the protein atoms with the 40 ns simulation time.

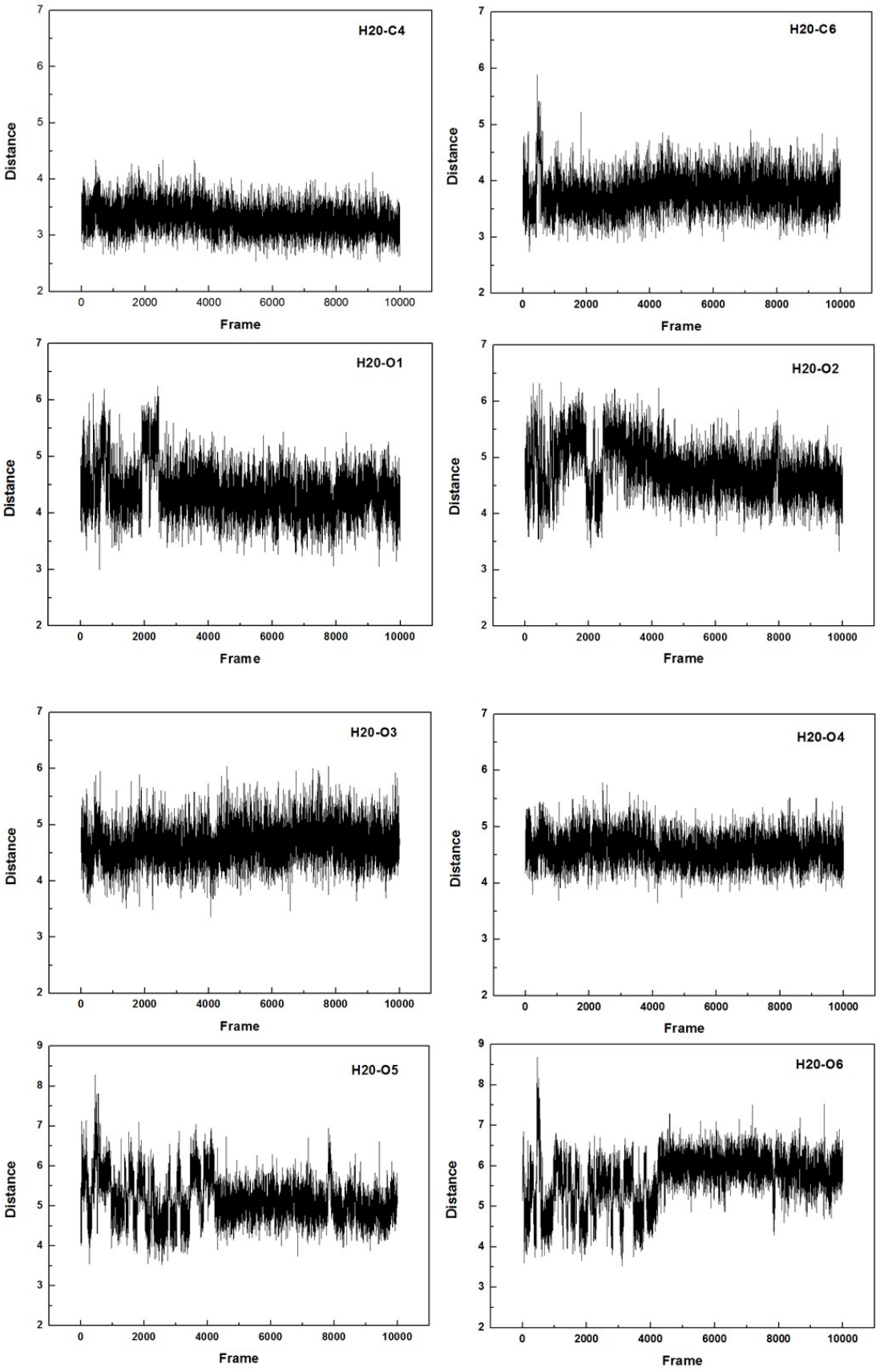

Figure S3. The curves of the distance of H_{20} to different transfer sites (C_4, C_6, O_1-O_6) on TNT during the whole 20 ns MD simulations.

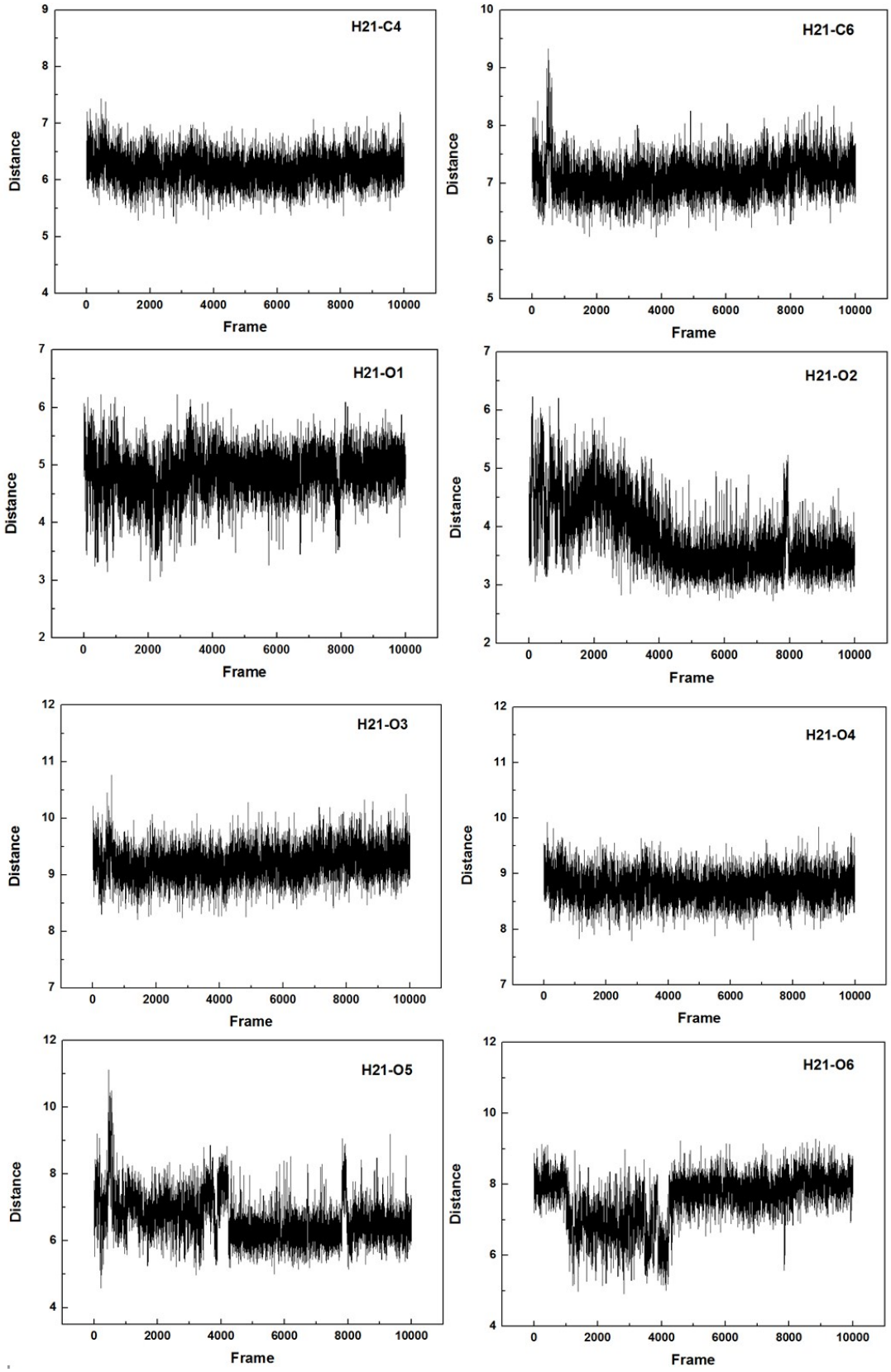

Figure S4. The curves of the distance of H_{21} to different transfer sites (C_4, C_6, O_1-O_6) on TNT during the whole 20 ns MD simulations.

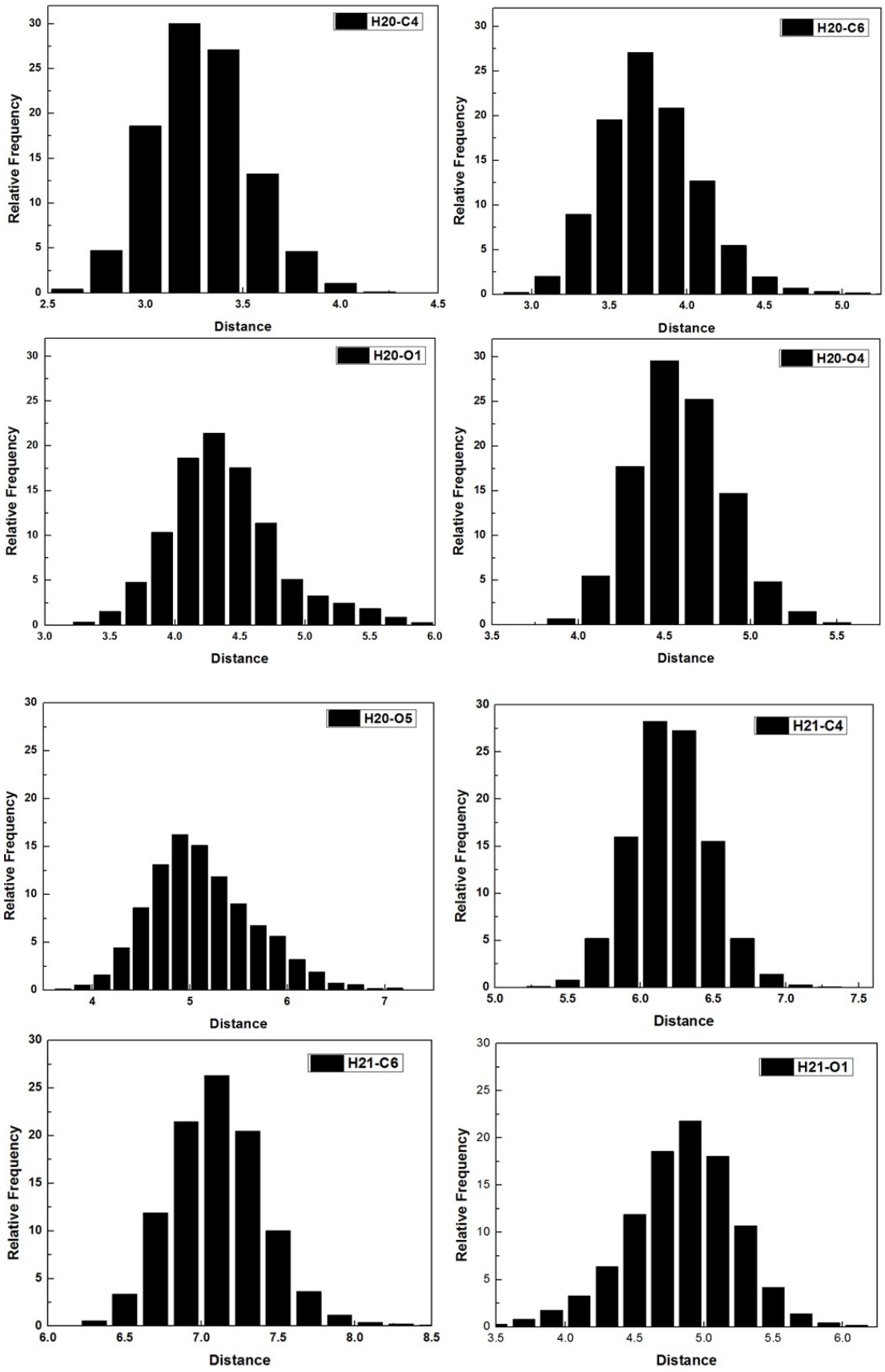
H20-C4
Relative Frequency
Distance
H20-C6
Relative Frequency
Distance
H20-O1
Relative Frequency
Distance
H20-O4
Relative Frequency
Distance
H20-O5
Relative Frequency
Distance
H21-C4
Relative Frequency
Distance
H21-C6
Relative Frequency
Distance
H21-O1
Relative Frequency
Distance

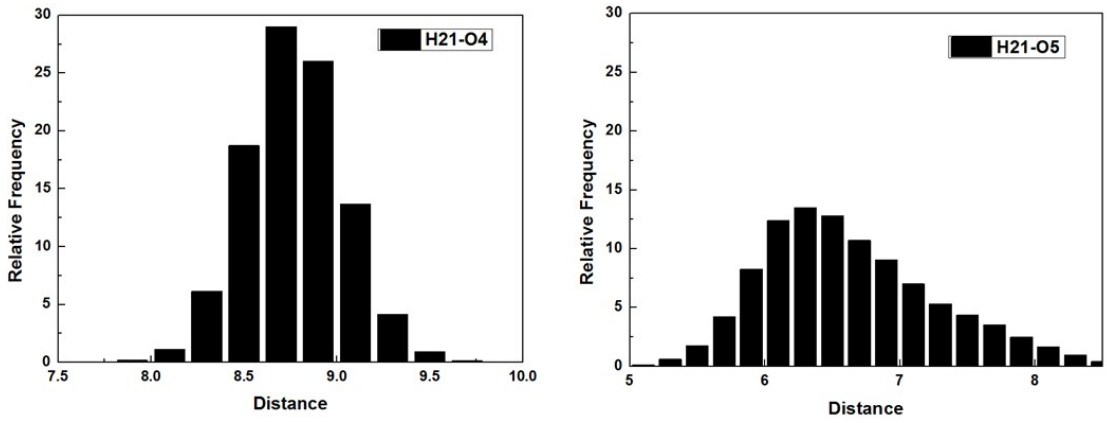

Figure S5. The mean distance and distribution of H_{20} and H_{21} respectively to the hydrogen transfer sites (C_4, C_6, O_1, O_4, O_5) on TNT during the whole 20 ns MD simulations

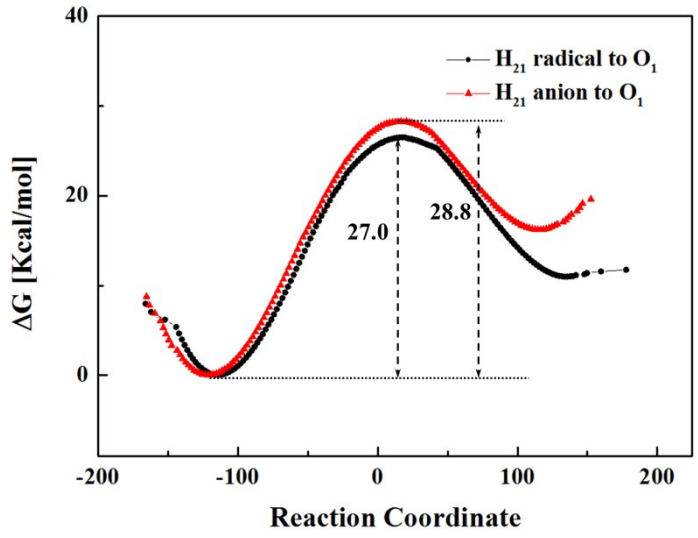

Figure S6. The free energy curves of the reactions of H_{21} radical and anion transfer to O_1 atom of TNT by EVB simulations. The barrier of H_{21} radical and anion to O_1 is 27.0 kacl/mol and 28.8 kacl/mol, respectively.

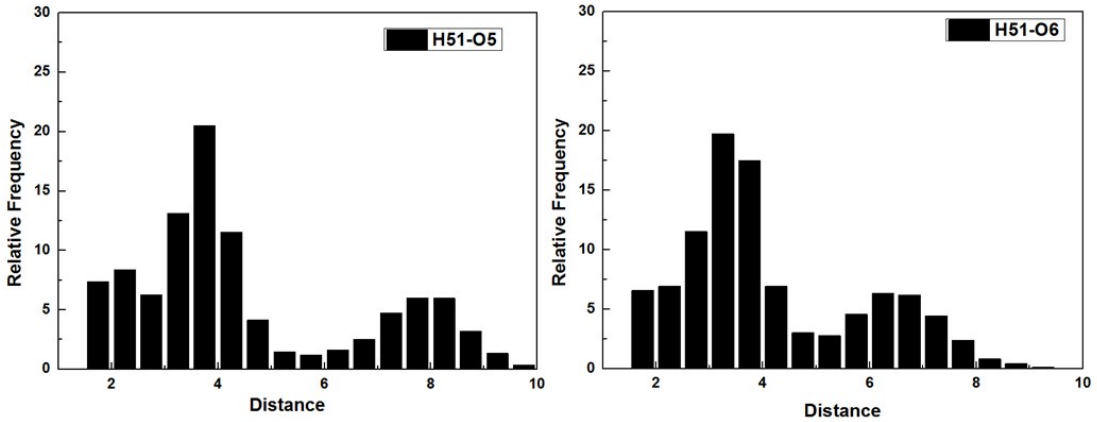

Distance	$H_{51}\ldots O_5$		$H_{51}\ldots O_6$	
Range/Å	1.55-6.00	6.00-10.30	1.51-5.00	5.00-9.81
Mean/Å	3.41 ±0.92	7.21 ±0.80	3.22±0.75	6.57±0.82
Percentage/%	74.06	25.96	72.08	27.92

Figure S7. The mean distance and standard deviation of H_{51}(Tyr351) to O_5 and O_6. The each graph shows two summits corresponding to two different mean distance in different conformations of Tyr351. The percentage of different ranges (different conformations) is also calculated.

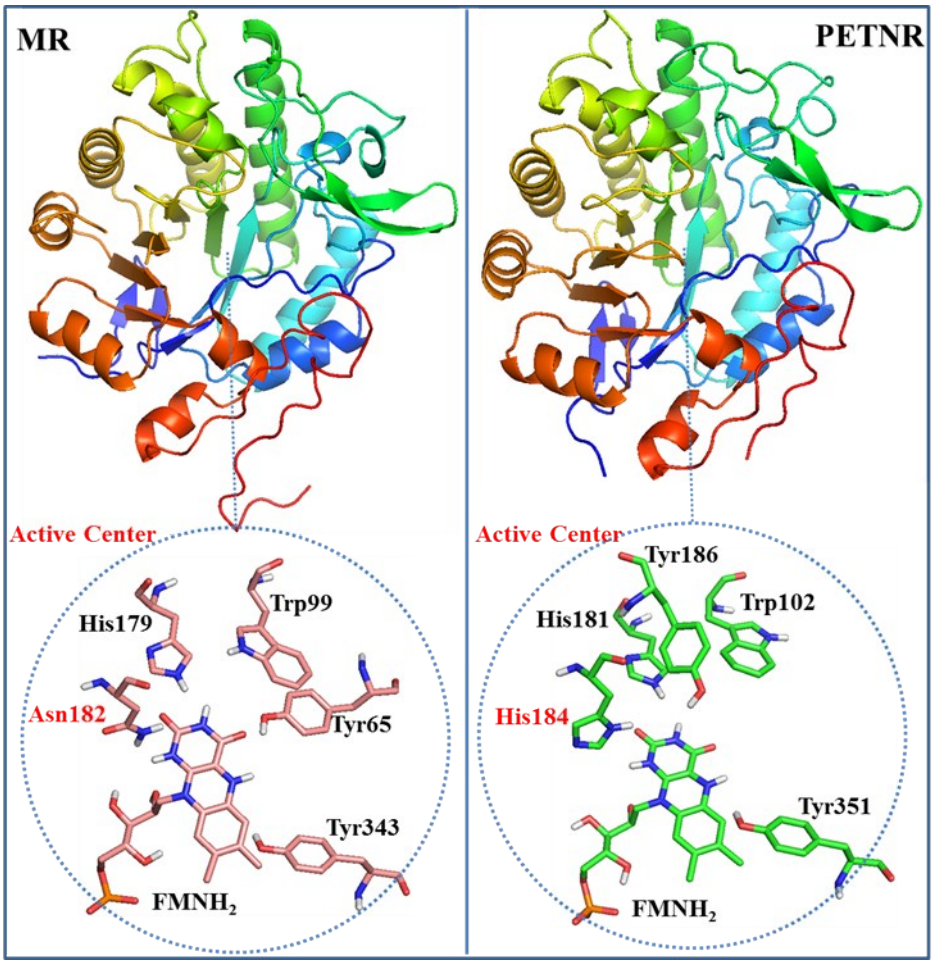

Figure S8. The overall structure comparison between PETNR and MR, especially the residues at the active sites.

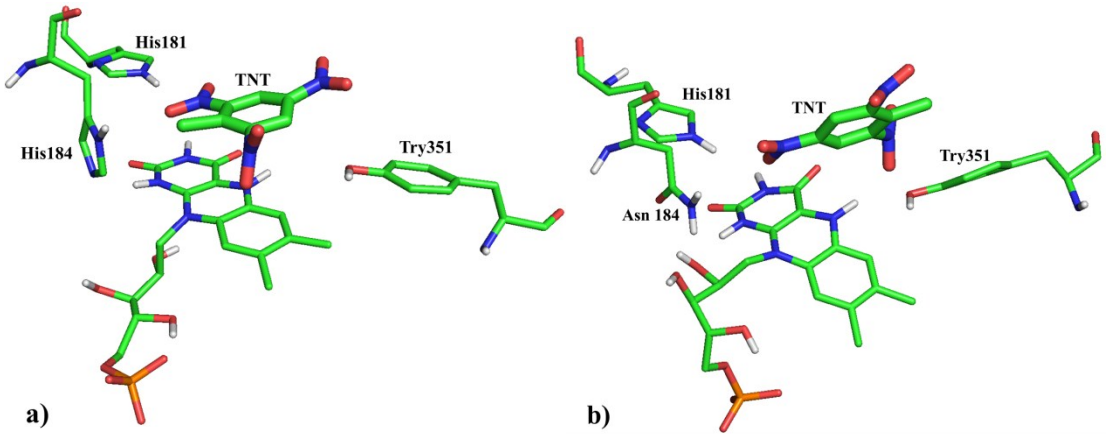

Figure S9. The comparison of the key residues (His184, Try351) between wild-type PETNR a) and His184Asn PETNR b) during the last 10 ns MD simulations.

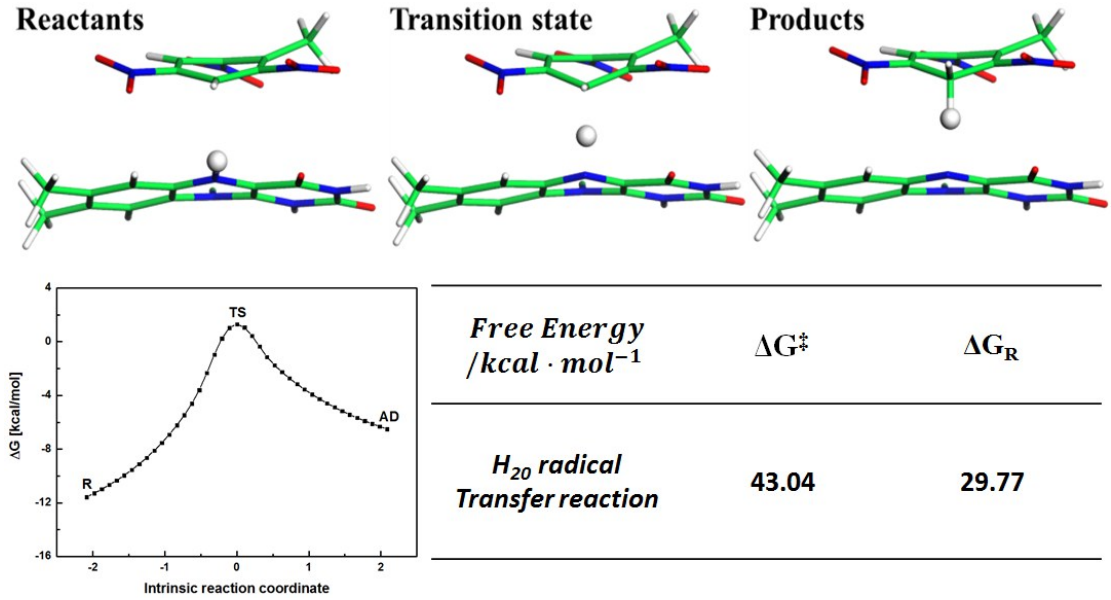

Free Energy $/kcal \cdot mol^{-1}$	$\Delta G^{\ddagger}$	ΔG_R
H_{20} radical Transfer reaction	43.04	29.77

Figure S10. H_{20} radical transfer step of TNT enzymatic reaction in the gas phase, and the intrinsic reaction coordinate (IRC) profile (B3LYP/6-31G* results) with the indicated stationary points corresponding to the reactant (R), transition state (TS), and product (P), and the correlative activation free energy ($\Delta G^{\ddagger}$) and reaction free engergy (ΔG_R).

Table S1. Coupling parameter and weights for 7-point Gaussian integration

n	1	2	3	4	5	6	7
λ_i	0.00000	0.04691	0.23076	0.50000	0.76923	0.95308	1.00000
ω_i	0.00000	0.11846	0.23931	0.28444	0.23931	0.11846	0.00000

Table S2. The mean distance and standard deviation of the residues polar hydrogen to oxygen of TNT in the PETNR active center.

Distance/Å	O_1	O_2	O_3	O_4	O_5	O_6
$H_{81}(His181)$	2.29 ± 0.33	2.65 ± 0.47				
$H_{51}(Tyr351)$			5.66 ± 1.29	7.48 ± 1.40	4.55 ± 2.13	4.15 ± 1.69
$H_{84}(His184)$	6.07 ± 0.89	4.47 ± 0.71			6.11 ± 1.03	6.49 ± 0.93
$H_{86}(Tyr186)$	4.76 ± 0.55	4.70 ± 0.61				
$H_{02}(Trp102)$	7.13 ± 0.68	8.76 ± 0.89	8.52 ± 0.64	6.49 ± 0.64		

Table S3. Non-bonded interactions energy (means and standard deviations) between residue 184 (or 351) and TNT of wild-type PETNR and His184Asn PETNR during the last 10 ns MD simulations. Elec: electrostatic energy; Vdw: van der waals energy; all the energy in kcal/mol.

Type of PETNR	Residues	Elec	Vdw	Vdw+Elec
wild-type	His184-TNT	0.76±0.84	-3.08±0.40	-2.32±0.89
	Try351-TNT	-0.51±1.01	-1.16±0.90	-1.68±1.66
His184Asn	Asn184-TNT	-1.03±0.48	-1.05±0.49	-2.07±0.80
	Try351-TNT	-2.98±1.08	-4.26±1.08	-7.24±1.75

Table S4. Condensed Fukui Functions of TNT. $Q_{(N)}$ is the Hirshfeld charge of TNT, $Q_{(N+1)}$ is the Hirshfeld charge of TNT combining an electron, and $Q_{(N-1)}$ is the Hirshfeld charge of TNT subtracting an electron. $f_A^0=(Q_{(N-1)}+Q_{(N+1)})/2$ corresponds to the ability of free-radical attack.

	$Q_{(N+1)}$	$Q_{(N)}$	$Q_{(N-1)}$	f_A^-	f_A^+	f_A^0
C4	-0.054627	-0.010347	0.081930	0.092277	0.044280	0.068279
C6	-0.054572	-0.010345	0.081876	0.092221	0.044227	0.068224
O1	-0.244115	-0.192240	-0.091465	0.100775	0.051875	0.076325
O2	-0.232123	-0.181826	-0.106583	0.075243	0.050297	0.062770